[21] Generation and Characterization of a Stable MK2-EGFP Cell Line and Subsequent Development of a High-Content Imaging Assay on the Cellomics ArrayScan Platform to Screen for p38 Mitogen-Activated Protein Kinase Inhibitors

By RHONDA GATES WILLIAMS, RAMANI KANDASAMY, DEBRA NICKISCHER, OSCAR J. TRASK, JR., CARMEN LAETHEM, PATRICIA A. JOHNSTON, and PAUL A. JOHNSTON

Abstract

This chapter describes the generation and characterization of a stable MK2-EGFP expressing HeLa cell line and the subsequent development of a high-content imaging assay on the Cellomics ArrayScan platform to screen for p38 MAPK inhibitors. Mitogen-activated protein kinase activating protein kinase-2 (MK2) is a substrate of p38 MAPK kinase, and p38-induced phosphorylation of MK-2 induces a nucleus to cytoplasm translocation (Engel *et al.*, 1998; Neininger *et al.*, 2001; Zu *et al.*, 1995). Through a process of heterologous expression of a MK2-EGFP fusion protein in HeLa cells using retroviral infection, antibiotic selection, and flow sorting, we were able to isolate a cell line in which the MK2-EGFP translocation response could be robustly quantified on the Cellomics ArrayScan platform using the nuclear translocation algorithm. A series of assay development experiments using the A4-MK2-EGFP-HeLa cell line are described to optimize the assay with respect to cell seeding density, length of anisomycin stimulation, dimethyl sulfoxide tolerance, assay signal window, and reproducibility. The resulting MK2-EGFP translocation assay is compatible with high-throughput screening and was shown to be capable of identifying p38 inhibitors. The MK2-EGF translocation response is susceptible to other classes of inhibitors, including nonselective kinase inhibitors, kinase inhibitors that inhibit upstream kinases in the p38 MAPK signaling pathway, and kinases involved in cross talk between different modules (ERKs, JNKs, and p38s) of the MAPK signaling pathways. An example of mining ''high-content'' image-based multiparameter data to extract additional information on the effects of compound treatment of cells is presented.

Introduction

There has been a growing trend in drug discovery toward the implementation of cell-based assays where the target is screened in a more physiological

METHODS IN ENZYMOLOGY, VOL. 414 0076-6879/06 $35.00

DOI: 10.1016/S0076-6879(06)14021-5

context than in biochemical assays of isolated targets (Johnston and Johnston, 2002). Fluorescence microscopy, confocal or wide field, is one of the most powerful tools that cell biologists have used to interrogate the amount and spatial temporal location of biomolecules that comprise the molecular mechanisms of the cell (Giuliano *et al.*, 1997; Mitchison, 2005). High-content screening (HCS) platforms automate the capture and analysis of fluorescent images of thousands of cells in the wells of microtiter plates with a throughput and capacity that has made fluorescence microscopy and image analysis compatible with drug discovery (Almholt *et al.*, 2004; Lundholt *et al.*, 2005; Oakley *et al.*, 2002; Ramm *et al.*, 2003). The ArrayScan was one of the first HCS platforms introduced to the drug discovery market by Cellomics, Inc. (Pittsburgh, PA) in 1997, and there are now more than a dozen models of HCS imagers on the market. By selection of the appropriate probes (antibodies, fluorescent protein fusion partners, biosensors, and stains), fluorescence microscopy can be applied to many drug target classes. HCS assays may be configured to simultaneously detect multiple target readouts (multiplexing) and can provide information on cellular morphology, population distributions, and subcellular localizations and relationships. Image-based assays provide multiparameter quantitative and qualitative information beyond the single parameter target data typical of most other assay formats, and thus are termed "high content" (DeBiasio *et al.*, 1987; Giuliano *et al.*, 1997; Mitchison, 2005).

The introduction of green fluorescent protein (GFP), and a variety of its spectral variants, into heterologous organisms has allowed cell biologists to monitor the dynamics of GFP-fusion proteins in living cells, thus addressing both temporal and spatial aspects (Giuliano and Taylor, 1998; Roessel and Brand, 2004; Tavare *et al.*, 2001). GFP and its variants have been used to study gene expression profiling, protein trafficking, protein translocation, lipid metabolism, protein–protein interactions, second messenger cascades (Ca^{2+}, cAMP, cGMP, and $InsP_3$), protein phosphorylation, proteolysis, intracellular ion concentrations, and intracellular pH (Giuliano and Taylor, 1998; Roessel and Brand, 2002; Tavare *et al.*, 2001). The combination of heterologous GFP-fusion protein expression with automated HCS imaging platforms has been utilized to screen a number of drug target classes: G-protein coupled receptors (GPCRs), kinase inhibitors, nuclear export inhibitors, signaling pathway inhibitors, and cell cycle targets (Almholt *et al.*, 2004; Lundholt *et al.*, 2005; Oakley *et al.*, 2002; Thomas and Goodyer, 2003). Automated imaging platforms are being deployed in many phases of the drug discovery process: target identification/target validation, primary screening and lead generation, hit characterization, lead optimization, toxicology, bio-marker development, diagnostic histopathology, and other clinical applications. The purpose of this chapter is to describe the generation and characterization of a stable mitogen-activated protein kinase-activated protein kinase-2 (MK2) enhanced-GFP

cell line (MK2-EGFP) and the subsequent development of a high-content imaging assay on the Cellomics ArrayScan automated imaging platform to screen for p38 MAPK inhibitors.

Definition of the Cell Model

Mitogen-activated protein (MAP) kinases are members of the signaling cascades for diverse extracellular stimuli that regulate fundamental cellular processes. Four distinct MAP kinase families have been described: extracellular signal-regulated kinases (ERKs), c-jun N-terminal (JNK) or stress-activated protein kinases (SAPK), ERK5/big MAP kinase 1 (BMK1), and the p38 group of protein kinases (Cowan and Storey, 2003; Garrington and Johnson, 1999; Ono and Han, 2000). p38 (reactivating kinases, RKs or p40) kinases are known to mediate stress responses and are activated by heat shock, ultraviolet light, bacterial lipopolysaccharide (LPS), or the proinflammatory cytokines interleukin (IL)-1β or tumor necrosis factor (TNF)-α (Cowan and Storey, 2003; Garrington and Johnson, 1999; Ono and Han, 2000). Activation of the p38 pathway results in phosphorylation of downstream kinases, transcription and initiation factors that affect cell division, apoptosis, invasiveness of cultured cells, and the inflammatory response (Cowan and Storey, 2003; Garrington and Johnson, 1999; Ono and Han, 2000). In addition to p38α (CSBP, MPK2, RK, Mxi2), there are three p38 homologues: p38β, p38γ (ERK6, SAPK3), and p38δ (SAPK4) (Ono and Han, 2000). p38α and p38β are expressed ubiquitously, p38γ is expressed predominantly in skeletal muscle, and p38δ is enriched in lung, kidney, testis, pancreas, and small intestine (Ono and Han, 2000). While p38 MAP kinase phosphorylates a number of transcription factors, including ATF2, CHOP/GADD153, and MEF2, it also activates many downstream protein kinases, such as the MAP kinase-activated protein kinases MK2 and MK3, the MAP-interacting kinases MNK1 and MNK2, and the p38-regulated/activated protein kinases PRAK and MSK1 (Cowan and Storey, 2003; Garrington and Johnson, 1999; Ono and Han, 2000). Selective inhibition of p38α-MAPK would be expected to inhibit production of TNF-α and IL-1β, as well as other proinflammatory mediators such as IL-6 and COX-2, thereby reducing the inflammation and/or joint destruction associated with rheumatoid arthritis (English and Cobb, 2002; Fabbro *et al.*, 2002; Noble *et al.*, 2004; Regan *et al.*, 2002). The hypothesis that p38 may be a potential drug target is a popular one, as indicated by the large number of patent applications (>48) that have been submitted by 15 pharmaceutical companies describing small molecule modulators of this pathway (English and Cobb, 2002; Regan *et al.*, 2002).

MK2 is a 370 amino acid Ser/Thr kinase with a proline-rich N terminus, a highly conserved catalytic domain, and a C-terminal region containing an

autoinhibitory A-helix (AH), a leucine-rich nuclear export signal (NES), and a functional nuclear localization signal (NLS) (Engel *et al.*, 1998; Neininger *et al.*, 2001; Zu *et al.*, 1995). The proline-rich N terminus of MK2 may interact with proteins that contain SH3 domains. In MK2 there are two regulatory phosphorylation sites: threonine 205 (T205), which is located at the activation loop of the kinase between subdomains VII and VIII, and threonine 317 (T317), which is adjacent to the autoinhibitory AH domain (Engel *et al.*, 1998; Neininger *et al.*, 2001; Zu *et al.*, 1995). Phosphorylation of T205 contributes to activation of the kinase by changing the conformation of the activation loop within the catalytic domain. Based on a number of deletion mutants and GFP fusion studies, a model has been proposed for the role of phosphorylation of T317 in MK2 activation and translocation from the nucleus to the cytoplasm (Engel *et al.*, 1998; Neininger *et al.*, 2001; Zu *et al.*, 1995). The NLS is accessible in the inactive and active form of the kinase, whereas the NES is only functional in the phosphorylated and activated form of the enzyme. It has been proposed that the inactive form of MK2 exists in a closed conformation that resides exclusively in the nucleus. Upon activation of the MAP kinase pathways by stress, p38-mediated phosphorylation of MK2 T317 produces a conformational switch to a more open form that activates the kinase by reducing the interaction between the AH and catalytic domains and demasks the overlapping NES. The unmasked NES of MK2 becomes accessible to exportin or an exportin-binding adaptor, and the activated kinase is exported rapidly from the nucleus. MK2 activation and its nuclear export are therefore coupled by this conformational opening. In the active state, both the NES and the NLS are accessible, but nuclear export appears to be more effective that its import, leading to a steady state where most of the continuously shuttling protein is cytoplasmic (Engel *et al.*, 1998; Neininger *et al.*, 2001; Zu *et al.*, 1995). MK2 is essential for LPS-induced TNFα biosynthesis (Kotlyarov *et al.*, 1999) and targets the AU-rich 3'-untranslated regions of the proinflammatory cytokines TNFα and IL-6, thereby regulating their biosynthesis (Neininger *et al.*, 2002).

We decided to generate a stable MK2-EGFP expressing cell line to take advantage of the p38-induced nucleus to cytoplasm translocation that could be quantified on an HCS imaging platform as a cell-based model for identifying inhibitors of p38.

Generation and Characterization of MK2-EGFP HeLa Cell Line

A MK2 clone obtained from colleagues at Lilly research laboratories (Indianapolis, IN) contains the cDNA described in GenBank #X75346. This cDNA sequence was originally amplified to contain the coding region from AA 32 to the end of the coding region of the GenBank entry.

An N-terminal truncated form of MK2 missing the first 31 amino acids was expressed in *Escherichia coli* and was utilized successfully as a p38 substrate for in gel kinase assays (data not shown). Because the regulatory p38 phosphorylation sites are contained in this clone and it is the C-terminal region that contains the T317 site, AH, NES, and NLS motifs (Engel *et al.*, 1998; Neininger *et al.*, 2001; Zu *et al.*, 1995), we decided to proceed with this truncated insert rather than generate a full-length clone. The pGEX/MK2 plasmid is digested with *Bam*H1 and *Xho*I, run on a 1% agarose gel, and the ~1.1-kb MK2 cDNA fragment was subcloned into the *Bgl*II/*Sal*I cut pLEGFPC1 retroviral vector. The pLEGFPC1/MK2 was transfected into Phoenix Amphotropic packaging cells, and retrovirus harvested 48 h post-transfection is used to infect HeLa (CCL-2, ATCC, Rockville, MD) cells.

Single-cell clones were isolated from a population of MK2-EGFP retrovirus-infected HeLa cells that were placed under selection with G418 48 h postinfection and sorted using the Beckman-Coulter Elite flow cytometer sorter equipped with an autoclone single-cell deposition device (Hialeah, FL). EGFP fluorescence was excited with a 15-mW 488-nm Ag laser, and emission was collected though 550-nm DCLP and 525-nm band-pass filter sets. Three distinct populations of cells based on cell size and EGFP fluorescent intensity, high, medium, or low, were isolated using the cell-sorting procedure. A number of cell clones were expanded in culture for 2 weeks under G418 selection conditions and characterized by FACS analysis (Fig. 1, Table I). Six separate flow-sorted clonal cell lines were compared for EGFP expression levels, fluorescent intensity, cell viability, and the robustness of their MK2-EGFP translocation responses on the ArrayScan (see later). For 9 of the 10 cell lines analyzed by FACS (Table I), the number of cells positive for EGFP expression ranges between 56 and 80%. For those same cell lines, the mean fluorescent intensity (MFI) of the EGFP signal was more varied, ranging between 70 and 266 MFI. The cell clone designated ''A4'' was 78% positive for EGFP expression with an MFI of 105 and was selected for further assay development (see later).

Fluorescence microscopy was used to analyze the subcellular distribution of MK2-EGFP in HeLa cells infected with the MK2-EGFP retrovirus (Fig. 2). The C2 stable population of HeLa-MK2-EGFP cells was seeded in four-well chamber slides, treated with ±100 n*M* anisomycin for 30 min, fixed with 3.7% formaldehyde containing Hoechst dye for 10 min, and examined on a Nikon Eclipse TE300 (Japan) fluorescence microscope equipped with a 300-W Hg lamp and GFP filter set (Chroma, Battlebrook, VT) (Fig. 2). Images were captured on a Micropublisher (Qimaging, Burnaby, BC, Canada) camera. In untreated cells, MK2-EGFP is predominantly located in the nucleus of the cells where it appears to colocalize with the nuclear Hoechst stain (Fig. 2).

Treatment with anisomycin induces the translocation of the majority of the MK2-EGFP into the cytoplasm (Fig. 2).

Cellomics ArrayScan Automated Imaging Platform

The largest category of HCS systems in the market place, and by far the largest installed base, is wide-field fixed cell imaging platforms. The ArrayScan platform marketed by Cellomics is one of the most widely

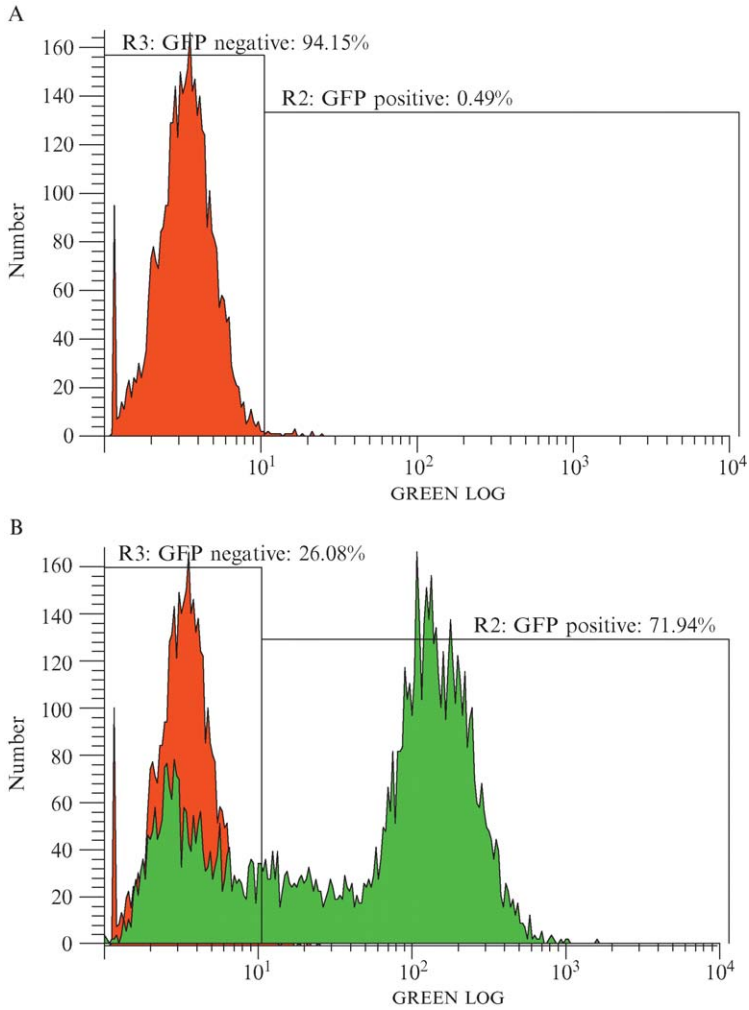

FIG. 1. (*continued*)

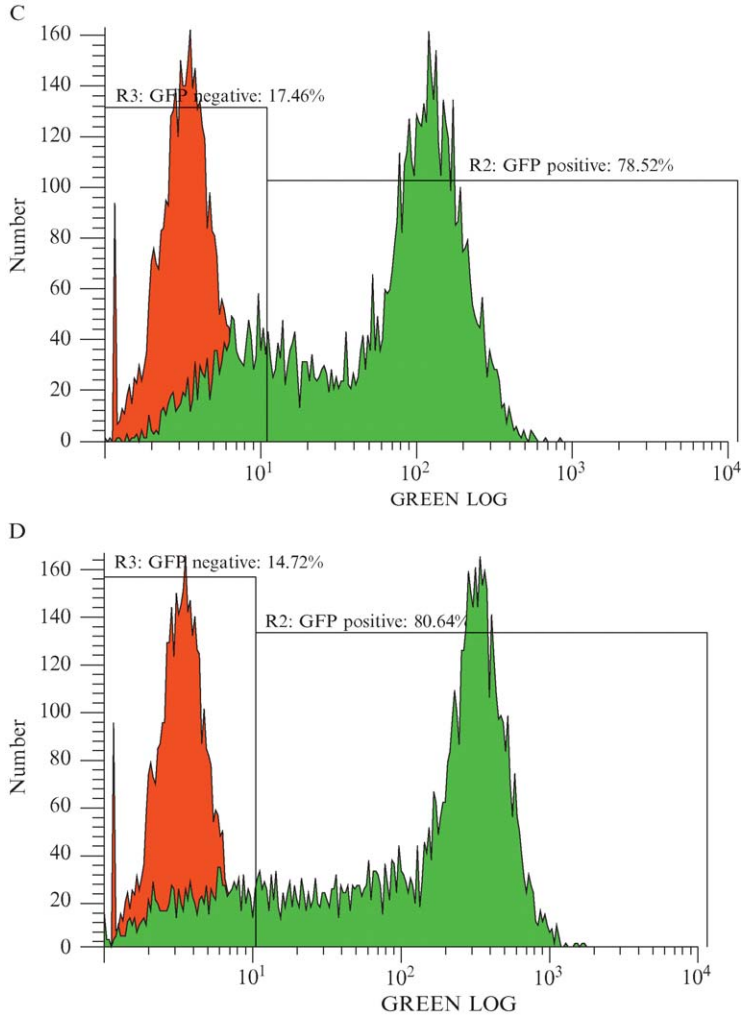

FIG. 1. FACS analysis of parental HeLa cells and MK2-EGFP-HeLa cell lines. MK2-EGFP retrovirus-infected HeLa cells were sorted using the Beckman-Coulter Elite flow cytometer sorter equipped with an autoclone single-cell deposition device (Hialeah, FL). EGFP fluorescence was excited with a 15-mW 488-nm Ag laser, and emission was collected though 550-nm DCLP and 525-nm BP filter sets. Three distinct populations of cells based on cell size and EGFP fluorescent intensity, high, medium or low, were isolated using the cell-sorting procedure. Several cell clones were expanded under G418 selection conditions for further FACS analysis. (A) Parental HeLa Cells ~0% EGFP positive with 0 MFI, (B) C1 stable infection with 71.94% EGFP positive and 123 MFI, (C) A4 clone 78.5% EGFP positive with 105 MFI, and (D) C5 clone 80.64% EGFP positive with 266 MFI.

TABLE I
FACS ANALYSIS OF FLOW SORTER-DERIVED MK2-EGFP CELL LINES

Clone	% GFP positive	MFI
C2 infected	74.64	136.51
C2-AO2 pool	78.46	101.79
C5	80.64	266.03
A4	78.52	105.54
F2	74.94	92.22
D7	74.6	136.09
D10	68.56	70.30
A7	63.92	175.11
C6	56.24	124.37
F5	18.66	19.90
Parental	0.68	NA

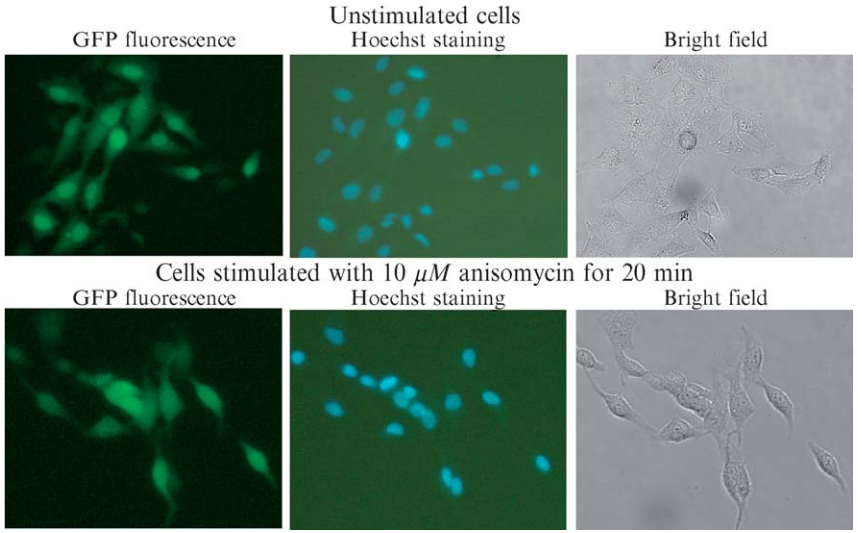

FIG. 2. Fluorescence and bright-field images of MK2-EGFP HeLa cells. HeLa-MK2-GFP infected cells were seeded in four-well chamber slides, treated with ±100 n*M* anisomycin for 30 min, fixed with 3.7% formaldehyde containing Hoechst dye for 10 min, and examined on a Nikon Eclipse TE300 (Japan) fluorescence microscope equipped with a 300-W Hg lamp and GFP filter set (Chroma, Battlebrook, VT). Images were captured on a Micropublisher (Qimaging, Burnaby, BC, Canada) camera.

deployed HCS systems. The studies described in this chapter are performed on an ArrayScan II that had the software upgraded to a 3.1 version. The ArrayScan 3.1 houses a Zeiss Axiovert S100 inverted microscope outfitted with 5×/0.25 NA, 10×/0.3 NA, and 20×/0.4 NA Zeiss objectives. Illumination is provided by a Xe/Hg arc lamp source (EXFO, Quebec, Canada), and fluorescence is detected by a 12-bit high sensitivity –20° cooled CCD camera (Photometrics Quantix). The ArrayScan 3.1 provides the capability of imaging multiwavelength fluorescence by acquiring wavelength channels sequentially in which each fluorophore is separately excited and detected on the chip of a monochromatic CCD camera. Channel selection is accomplished using a fast excitation filter wheel combined with a multiband emission filter, although single band emission filters can be used to improve selectivity. The system comes with filter sets designed for the common fluorescent probes and can distinguish up to four labels in a single preparation with minimal cross talk between channels. The ArrayScan 3.1 was a wide-field imaging system that illuminates a ''large'' area of the specimen and directly images that area all at once. It uses an image-based autofocus system that images a fluorescent label in cells, typically fluorescently stained nuclei, but any feature of interest could be used, and an algorithm measures the relative sharpness of the image. The ArrayScan 3.1 was integrated with a Zymark Twister Robot and 80 plate stacker for fixed end point assays.

The cytoplasm-to-nuclear translocation algorithm developed by Cellomics may be used to quantify the relative distribution of a fluorescently tagged target between two cellular compartments, namely the cytoplasm and the nucleus (Giuliano *et al.*, 1997). Labeling with a nucleic acid dye such as Hoechst 33342, DAPI, or DRAQ5 identifies the nuclear region, and this signal is used to focus the instrument and to define a nuclear mask. The mask is eroded to reduce cytoplasmic contamination within the nuclear area, and the final reduced mask is used to quantify the amount of target channel fluorescence within the nucleus. The nuclear mask is then dilated to cover as much of the cytoplasmic region as possible without going outside the cell boundary. Removal of the original nuclear region from this dilated mask creates a ring mask that covers the cytoplasmic region outside the nuclear envelope. The ''Cytonuc'' difference measurement is calculated as the difference of the average nuclear intensity minus the average cytoplasmic ring intensity on a per cell basis or may be reported as an overall well average value (Giuliano *et al.*, 1997).

Characterization of MK2-EGFP Clones via Imaging

The Cellomics ArrayScan 3.1 was used to analyze the subcellular distribution of MK2-EGFP in HeLa cells infected with the MK2-EGFP retrovirus.

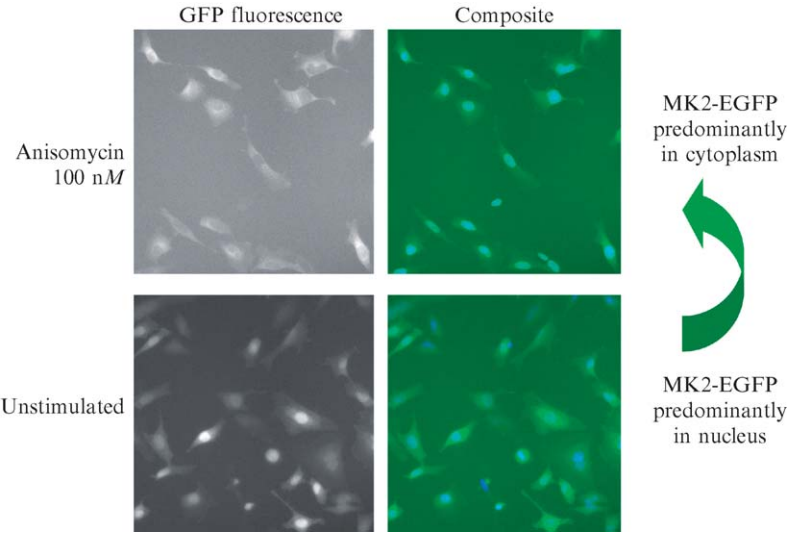

FIG. 3. Fluorescence images of MK2-EGFP HeLa cells captured on the ArrayScan. HeLa-MK2-EGFP A4 cells (5×10^3) were seeded into each of the 96-wells of Packard View plates in EMEM + 10% FBS and incubated overnight at 37° and 5% CO_2. Cells were treated ± 100 n*M* of anisomycin for 25 min and fixed in 3.7% formaldehyde + 2 μg/ml Hoechst dye, and fluorescent images were collected on the ArrayScan 3.1.

HeLa-MK2-EGFP A4 cells (5×10^3) per well were seeded in EMEM + 10% fetal bovine serum (FBS) and incubated overnight at 37° and 5% CO_2. Cells were either treated with 100 n*M* of the protein synthesis inhibitor anisomycin for 25 min or were left untreated and fixed in 3.7% formaldehyde +2 μg/ml Hoechst dye, and fluorescent images were collected on the ArrayScan 3.1 (Fig. 3). Consistent with the fluorescent images in Fig. 2, in untreated cells, MK2-EGFP is located predominantly in the nucleus and appears to colocalize with the Hoechst stain (Fig. 3). Treatment with anisomycin induces the translocation of the majority of the MK2-EGFP into the cytoplasm (Fig. 3). To compare the translocation responses of the different stable cell populations and flow-sorting derived clones (Fig. 1, Table I), anisomycin-induced translocation dose–response curves were run in triplicate (Fig. 4). Using the nuclear translocation algorithm to analyze images captured on the ArrayScan 3.1, the A4 clone and the C2 retroviral-infected population produced the most robust dose-dependent assay signal window (Fig. 4). The A4 clone was selected for further assay development.

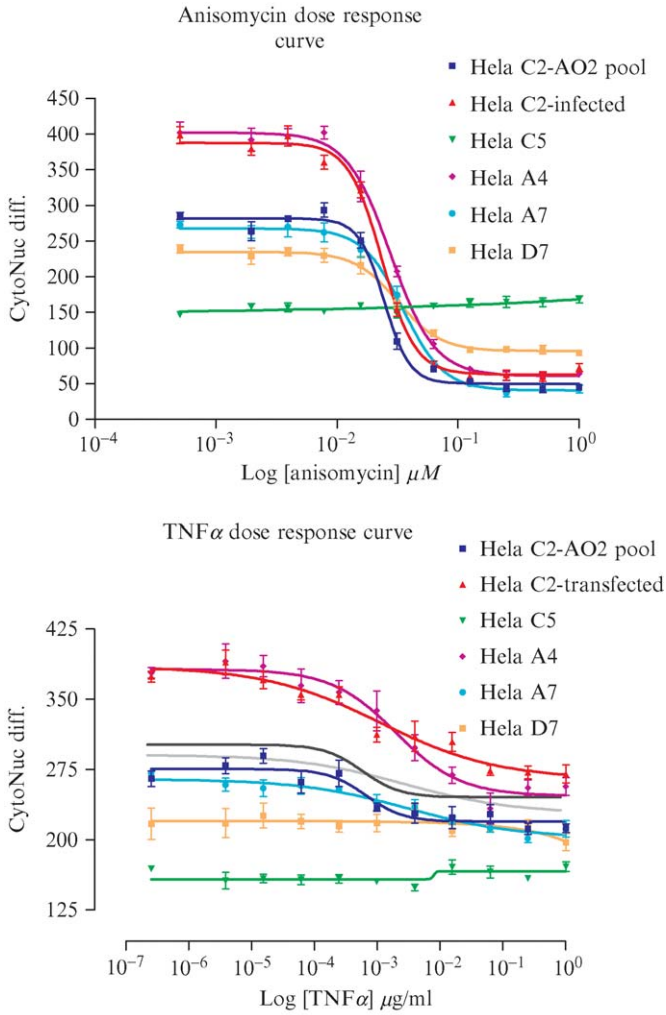

FIG. 4. Comparison of the anisomycin-induced nucleus to cytoplasm MK2-EGFP translocation responses in different flow-sorted cell populations quantified by the nuclear translocation algorithm from images captured on the ArrayScan. To compare the translocation responses of the different stable cell populations and flow-sorting-derived autoclones (Fig. 1, Table I), anisomycin-induced translocation dose–response curves were run in triplicate. HeLa-MK2-EGFP cells (5×10^3) from the indicated cell lines were seeded into each of the 96 wells of Packard View plates in EMEM + 10% FBS and incubated overnight at 37° and 5% CO_2. Cells were treated with the indicated doses of anisomycin for 25 min and fixed in 3.7% formaldehyde + 2 μg/ml Hoechst dye, and fluorescent images were collected on the ArrayScan 3.1. The nuclear translocation algorithm was used to analyze the images captured on the ArrayScan 3.1 and quantify the anisomycin-induced translocation response.

Characterization of the p38 MAPK Signaling Pathway in HeLa-MK2-EGFP Cells

To confirm that the p38 MAPK signaling pathway in the HeLa-MK2-EGFP-A4 clone is intact and similar to wild-type HeLa cells, both cell populations were treated with 100 n*M* anisomycin for 30 min. Cells were then solubilized in SDS sample buffer, their total cellular proteins were separated on 10% SDS-PAGE gels, transferred to nitrocellulose, and the resulting blots were probed with specific antibodies for total and phosphorylated p38 and MK-2 (Fig. 5). The total p38 signal detected on Western blots appears identical in both HeLa-MK2-EGFP-A4 population and wild-type HeLa cells and is unaffected by anisomycin treatment. In contrast, although the A4 clone and wild-type HeLa cells both exhibit a weak endogenous total MK2 signal at the appropriate molecular mass of ~45.5 kDa, the A4 cells also express a much stronger immunoreactive total MK2 signal at ~75 kDa, corresponding to 45 kDa MK2 plus the additional 30 kDa contributed by the EGFP fusion partner. Neither the endogenous MK2

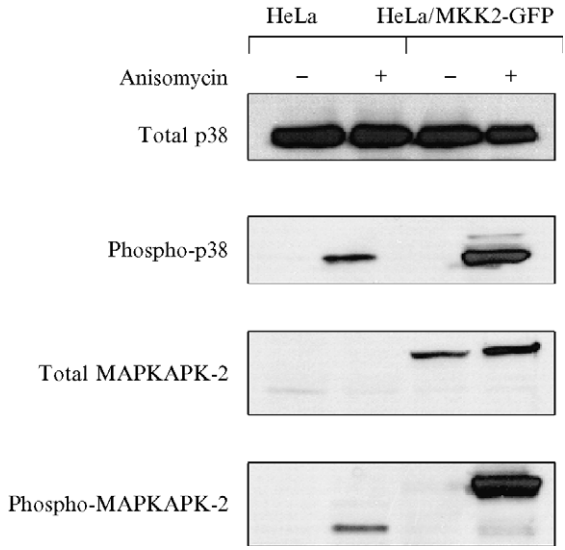

FIG. 5. Comparison of total and phosphorylated p38 and MK2 expression in parental HeLa and MK2-EGFP-HeLa A4 cells by Western blotting analysis. Parental HeLa cells and cells from the HeLa-MK2-EGFP-A4 clone were treated ± 100 n*M* anisomycin for 30 min. Cells were then solubilized in SDS sample buffer, their total cellular proteins were separated on 10% SDS-PAGE gels, transferred to nitrocellulose, and the resulting blots were probed with specific antibodies for total and phosphorylated p38 and MK-2.

nor the MK2-EGFP total protein signals are affected by anisomycin treatment. Activation of the p38 MAPK signaling pathway by anisomycin treatment dramatically increases the phosphorylation signals for p38 and MK2 in both cell populations relative to untreated controls. As expected from the total MK2 signals, the phospho-MK2 signal is stronger in the A4 clone relative to wild-type HeLa cells, and the majority of the immunoreactive signal migrates at the higher molecular mass of ~75 kDa. Interestingly, there is a stronger phospho-p38 signal apparent in the A4 clone relative to wild-type HeLa. In the A4 clone, overexpression of the MK2-EGFP fusion protein has no apparent effect on the qualitative pattern of the p38 and MK2 phosphorylation responses to activation by anisomycin, despite an overall increase in signal strength (Fig. 5).

Assay Development on the ArrayScan 3.1 Imaging Platform

Treatment of MK2-EGFP HeLa cells with 100 ng/ml anisomycin produces a significantly larger MK2-EGF translocation response than treatment with 50 ng/ml TNF-α when quantified on the ArrayScan 3.1 (Fig. 6A and B). However, the time course of MK2-EGFP export from the nucleus appears similar for both stimuli (Fig. 6A). The amount of MK2-EGFP that translocates from the nucleus to the cytoplasm appears to increase in a roughly linear fashion for 20 to 25 min post stimulation and then remains stable for as long as 90 min (Fig. 6A). A 25-min period of stimulation with anisomycin (100 ng/ml) was selected as the standard treatment to induce maximal MK2-EGFP translocation. The observed time course for MK2-EGFP translocation is consistent with published data (Engel *et al.*, 1998.). Seeding densities between 0.5 and 16×10^3 A4 cells per well produce fairly comparable MK2-EGFP translocation responses (Fig. 6B) for both stimuli. A seeding density of 5×10^3 cells per well was selected for the remaining assay development effort. Because compound-screening libraries are typically solubilized in dimethyl sulfoxide (DMSO), we evaluated the DMSO tolerance of the MK2-EGFP translocation response in A4 cells that were treated for 25 min with media, 100 ng/ml anisomycin, or 50 ng/ml TNF-α at the indicated DMSO concentrations (Fig. 6C). The MK2-EGFP translocation response appears unaffected at DMSO concentrations $\leq 0.65\%$. However, at DMSO concentrations $\geq 1.25\%$, irrespective of the stimulus, the Cytonuc difference was increased. At DMSO concentrations $\geq 1.25\%$, the majority of the A4 cell population assumes a rounded morphology rather than the well-attached, flat morphology more typical of this clone (Figs. 2 and 3). The rounded A4 cells have a much smaller cytoplasmic area than normal, and the Cytonuc difference algorithm therefore has difficulty segmenting the cytoplasm and nuclear areas to make the difference calculation.

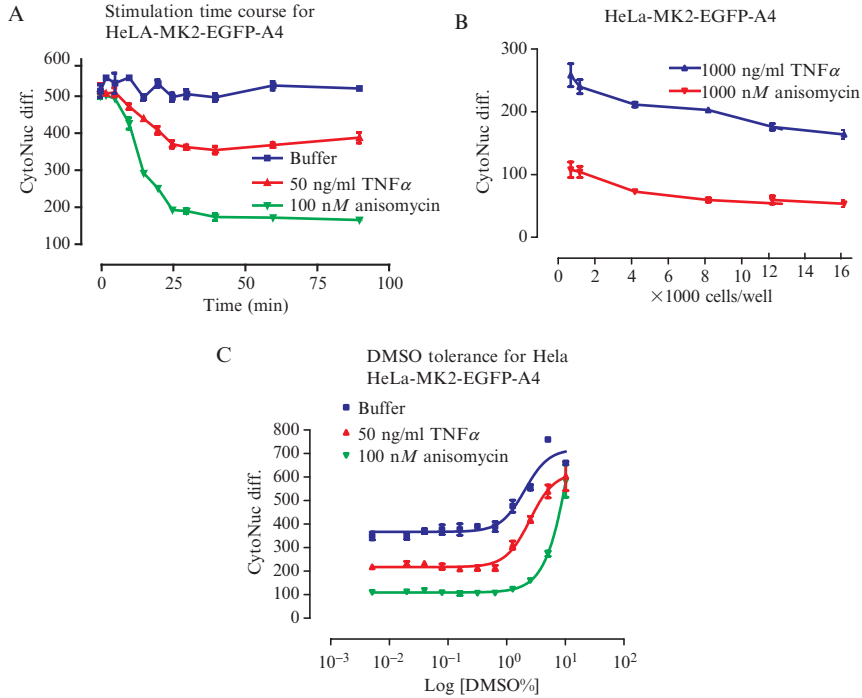

FIG. 6. MK2-EGFP translocation assay development. (A) Stimulation time course. HeLa-MK2-EGFP cells (5×10^3) from the HeLa-MK2-EGFP-A4 clone were seeded into each of the 96 wells of Packard View plates in EMEM + 10% FBS and incubated overnight at 37° and 5% CO_2. Cells were treated ± 100 ng/ml anisomycin or ± 50 ng/ml TNFα for the indicated times and fixed in 3.7% formaldehyde + 2 μg/ml Hoechst dye, and fluorescent images were collected on the ArrayScan 3.1. (B) Cell-seeding density. The indicated numbers of cells from the HeLa-MK2-EGFP-A4 clone were seeded into each of the 96 wells of Packard View plates in EMEM + 10% FBS and incubated overnight at 37° and 5% CO_2. Cells were treated ± 100 ng/ml anisomycin or ± 50 ng/ml TNFα for 25 min and fixed in 3.7% formaldehyde + 2 μg/ml Hoechst dye, and fluorescent images were collected on the ArrayScan 3.1. (C) DMSO tolerance. HeLa-MK2-EGFP cells (5×10^3) from the HeLa-MK2-EGFP-A4 clone were seeded into each of the 96 wells of Packard View plates in EMEM + 10% FBS and incubated overnight at 37° and 5% CO_2. Cells were treated ± 100 ng/ml anisomycin or ± 50 ng/mL TNFα containing the indicated concentrations of DMSO for 25 min and fixed in 3.7% formaldehyde + 2 μg/ml Hoechst dye, and fluorescent images were collected on the ArrayScan 3.1. The nuclear translocation algorithm was used to analyze the images captured on the ArrayScan 3.1 and quantify the anisomycin and TNFα-induced translocation response.

Standard Operating Procedure for the MK2-EGFP Translocation Assay

1. Sub-confluent HeLa-MK2-EGFP-A4 monolayers (70–80%) are detached from tissue culture flasks with trypsin-versene and centrifuged for 5 min at 800*g*.

2. Cells are resuspended in complete media (EMEM + 10% FBS + 2 m*M* L-glutamine + penicillin/streptomycin + 800 μg/ml G418) to a cell density to 5×10^4 cells/ml and seeded into 96-well Packard View plates using the Multidrop (Titertek, Huntsville, AL) at 100 μl/well (5000 cells/well).

3. Plates are incubated at 37°, 5% CO_2 and 95% humidity for 18 to 24 h.

4. Twenty-five microliters of compounds and controls are transferred to the wells of assay plates using a 96-well head on the Multimek (Beckman, Fullerton, CA), and plates are incubated at 37°, 5% CO_2, and 95% humidity for 12 min.

5. Twenty-five microliters of anisomycin (100 ng/ml final concentration) is transferred to the assay wells using a 96-well head on the Multimek, and plates are incubated at 37°, 5% CO_2, and 95% humidity for 25 min.

6. Plates are fixed by the addition of 150 μl of (37°) formaldehyde (3.7% final) + 2 μg/μl Hoechst 33342 stain using the Multidrop (Titertek) and incubated at room temperature in a fume hood for 12 min.

7. The fixation solution is aspirated, 100 μl of phosphate-buffered saline (PBS) is added to wash the monolayers, the PBS is aspirated, another 100 μl of PBS is added, and plates are sealed. This aspiration and wash process is performed on a MAP C2 96-well plate handler (Titertek).

8. Images are acquired on the ArrayScan 3.1 platform, and MK2-EGFP translocation is analyzed using the cytoplasm-to-nucleus translocation algorithm.

MK2-EGFP Translocation Assay Reproducibility and Signal Widow Evaluation

To evaluate the reproducibility of the MK2-EGF translocation response in A4 cells, EC_{50} values for anisomycin are determined in three independent experiments run on separate days (Fig. 7A). The EC_{50} for anisomycin-induced MK2-EGFP translocation ranged from 27 to 32 n*M* and produced, on average, an EC_{50} of 29.54 $\pm$ 2.75 nm, indicating that the translocation response was very reproducible.

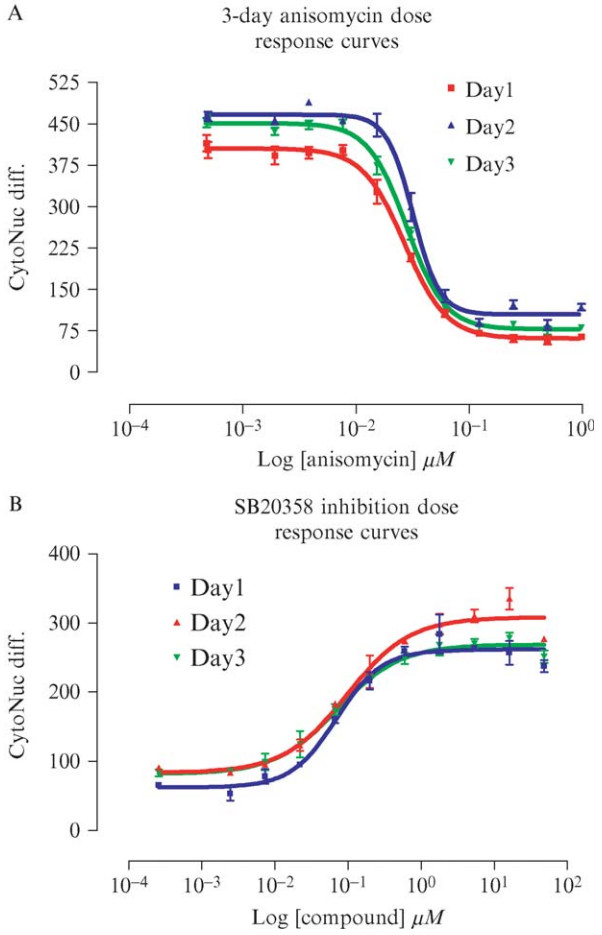

FIG. 7. Three-day MK2-EGFP translocation activation and inhibition curves. (A) Three-day EC_{50} curves. HeLa-MK2-EGFP-A4 cells were seeded at 5×10^3 cells per well in Packard View plates and on the following day were treated with the indicated doses of anisomycin for 25 min and fixed in 3.7% formaldehyde + 2 μg/ml Hoechst dye, and fluorescent images were collected on the ArrayScan 3.1. The nuclear translocation algorithm was used to analyze the images and quantify the anisomycin-induced translocation response. Data are presented from three independent experiments, each performed in triplicate wells and run on separate days. (B) Three-day IC_{50} curves. HeLa-MK2-EGFP-A4 cells were seeded at 5×10^3 cells per well in Packard View plates and on the next day were pretreated with the indicated doses of SB203580 for 12 min, followed by the addition of 100 ng/ml anisomycin (final) and a further incubation for 25 min. Plates were fixed in 3.7% formaldehyde + 2 μg/ml Hoechst dye, and fluorescent images were collected on the ArrayScan 3.1. The nuclear translocation algorithm was used to analyze the images and quantify the anisomycin-induced translocation response. Data are presented from three independent experiments, each performed in triplicate wells and run on separate days.

To examine the reproducibility of inhibition of the translocation response, three independent experiments are run on three separate days. On the day after seeding, cells are pretreated with the indicated doses of the p38 inhibitor SB203580 for 12 min, followed by the addition of 100 ng/ml anisomycin (final) and a further incubation for 25 min (Fig. 7B). The IC_{50} for SB203580 inhibition of anisomycin-induced MK2-EGFP translocation ranged from 72 to 99 n*M* and produced, on average, an IC_{50} of 82.12 $\pm$ 15.21 nm, indicating that the inhibition was reproducible.

Finally, the robustness of the MK2-EGF translocation response is quantified in full plate assays used to determine the *Z* factor (Zhang *et al.*, 1999). Three 96-well plates are treated under the following conditions: media alone (blue squares), 100 ng/ml anisomycin (red triangles), and p38 inhibitor + 100 ng/ml anisomycin (green circles) (Fig. 8). A comparison of either the media control plate or p38 inhibitor plate data to anisomycin plate data produced a *Z* factor (Zhang *et al.*, 1999) of 0.61 and an average assay signal window of 3.6-fold, indicating a good reproducible assay compatible with HTS.

p38 Inhibitor Data

Because p38 is an attractive target for anti-inflammatory and anticancer therapies, a number of pharmaceutical companies have developed p38 inhibitor compounds (English and Cobb, 2002; Fabbro *et al.*, 2002; Noble *et al.*, 2004; Regan *et al.*, 2002). In addition to five "selective" p38 inhibitors, we included a number of other kinase inhibitors to evaluate the selectivity of the MK2-EGF translocation response (Table II). The SP 600125 compound is a JNK-1/2 inhibitor, UO126 and PD 98059 are MEK-1/2 inhibitors, wortmannin is a PI3-kinase inhibitor, and staurosporin is a nonselective kinase inhibitor. All five p38 inhibitors produced IC_{50} values for inhibition of anisomycin-induced MK2-EGFP translocation <100 n*M*. Neither the PI3-kinase inhibitor wortmannin nor the JNK-1/2 inhibitor SP 600125 inhibited anisomycin-induced MK2-EGFP translocation. UO126 and PD 98059, the MEK-1/2 inhibitors, produced IC_{50} values of 33 and 39 μM respectively, while the nonselective kinase inhibitor staurosporin produced an IC_{50} of 0.75 μM (Fig. 7B, Table II).

Secondary Analysis Parameters

In addition to the target readout for nucleus to cytoplasm translocation, the algorithm provides a range of image-derived features at the individual cell level or at the well averaged level (Table III). These image-derived features provide information on cell morphology, cytotoxicity, and potential fluorescent artifacts produced by fluorescent compounds. The ArrayScan

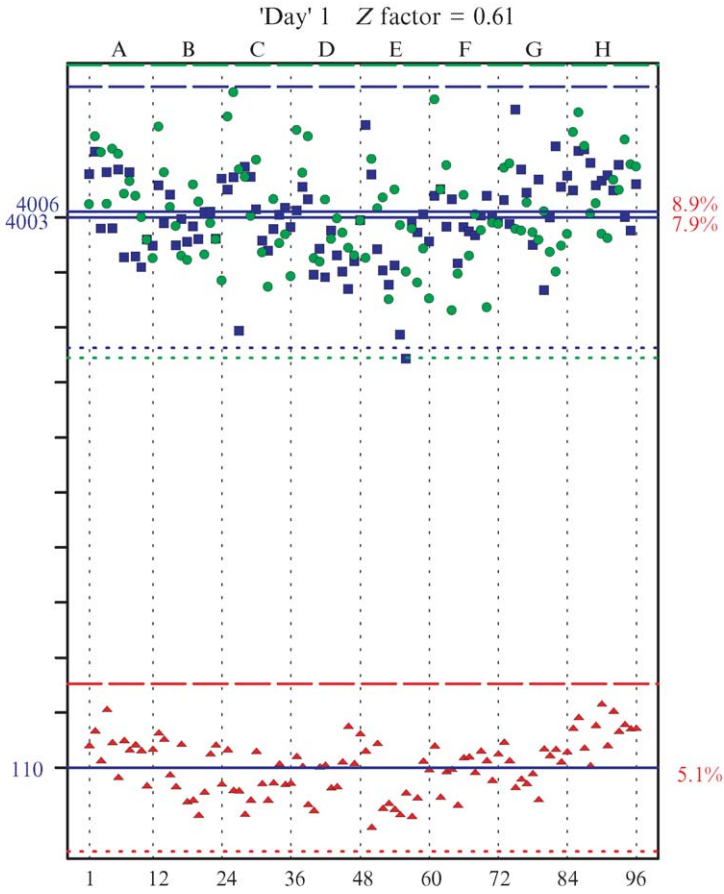

FIG. 8. Assay signal window and variability analysis of the MK2-EGFP translocation assay. HeLa-MK2-EGFP cells (5×10^3) from the HeLa-MK2-EGFP-A4 clone were seeded into each of the 96 wells of Packard View plates in EMEM + 10% FBS and incubated overnight at 37° and 5% CO_2. One full 96-well plate was treated for 25 min under the following conditions: media alone (blue squares), 100 ng/ml anisomycin (red triangles), and p38 inhibitor + 100 ng/ml anisomycin (green circles). Plates were fixed in 3.7% formaldehyde + 2 μg/ml Hoechst dye, and fluorescent images were collected on the ArrayScan 3.1. The nuclear translocation algorithm was used to analyze the images and quantify the anisomycin-induced translocation response. The *Z* factor was calculated according to the method of Zhang *et al.* (1999).

software provides data visualization tools that allow the user to analyze these multiparameter data and the images from which they are derived (Fig. 9). During the course of the p38 inhibitor studies described earlier (Table II, Fig. 7B), we observed that the two highest concentrations of the

TABLE II
MK2-EGFP KINASE INHIBITOR IC_{50} COMPARISON

Compound	Anisomycin	
	% Inhibition at 50 μM	IC_{50} μM
SP600125	29.5	>50
VX-745	146	0.045
Merch p38 inhib	−30.5	0.007
RWJ 68354	122	0.087
SB242235	96.5	0.028
SB203580	64	0.053
PD98059	58.5	39.000
U0126 # 9903	64	33.000
Wortmannin	33.5	>50
Staurosporin	180.5	0.755

TABLE III
CELL AND WELL FEATURES DERIVED BY THE NUCLEAR TRANSLOCATION IMAGE ANALYSIS ALGORITHM

Cell features	Well features
Nuc Area	Valid Object Count
Nuc Perimeter/Area	Selected Object Count
Nuc Area / Bounding Box	% Selected Object Count
Nuc Length / Width	Mean Nuc Area
Nuc Intensity (Nuc Ch)	Mean Nuc Intensity
Nuc Total Intensity (Nuc Ch)	Mean Nuc-Cyto Intensity Diff
Nuc Area (Target Ch)	Avg Cell Density/Field
Nuc Intensity (Target Ch)	Mean Nuc Intensity(Target Ch)
Nuc Total Intensity (Target Ch)	Mean Cyto Ring Intensity(Target Ch)
Cyto Ring Area (Target Ch)	Number of Valid Fields
Cyto Intensity (Target Ch)	Z-position
Cyto Total Intensity (Target Ch)	*CV & StdDev of features*
Nuc-Cyto Intensity Diff (Target Ch)	
Object Intensity / Area Ch2 – Ch6	
Object Total Intensity Ch2 – Ch6	

Merck p38 inhibitor compound, 50 and 16.6 μM, were producing obvious outliers in several of these parameters: the valid object counts, the average cell density per field, and the number of valid fields (Fig. 9A). A visual inspection of the images captured in these wells revealed that there were fewer cells in wells treated with 50 and 16.6 μM of the Merck inhibitor compared to the 5.5 μM dose or images from control wells (Fig. 9B). It is

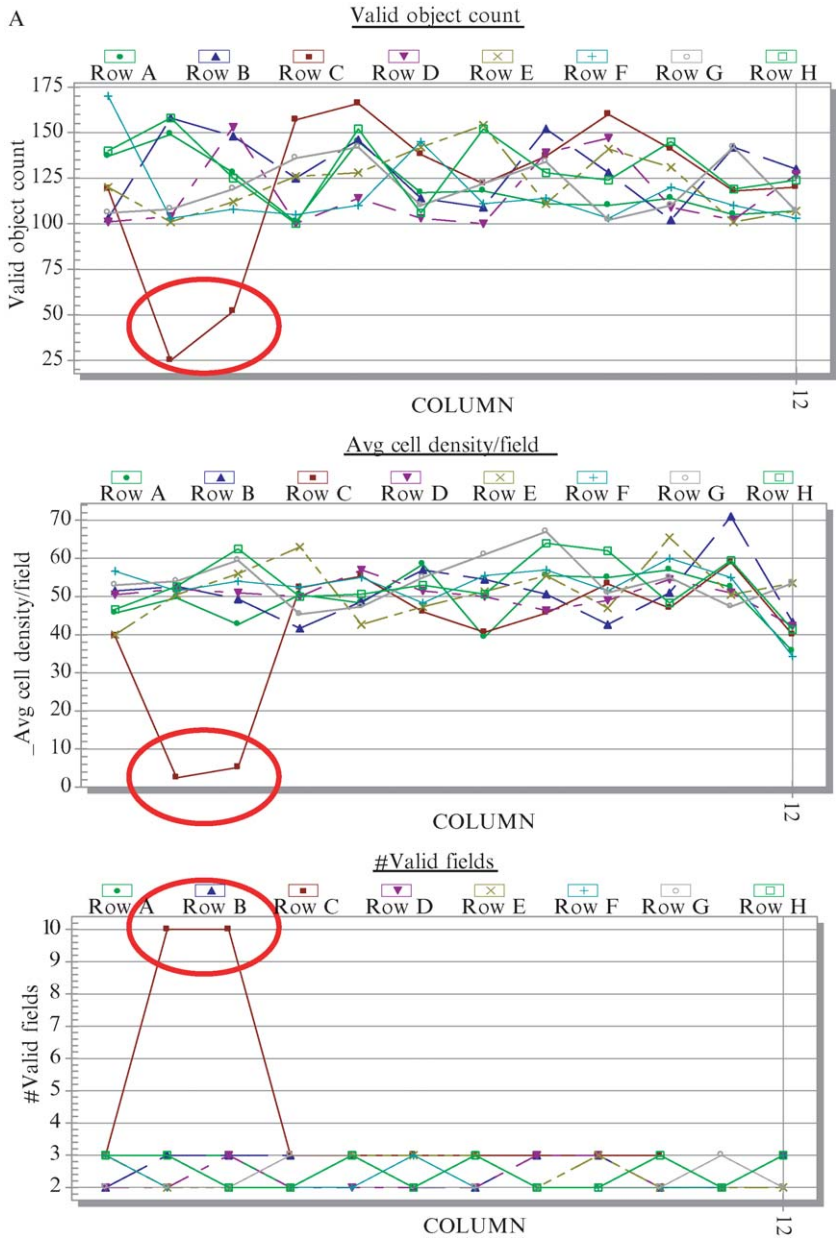

FIG. 9. (*continued*)

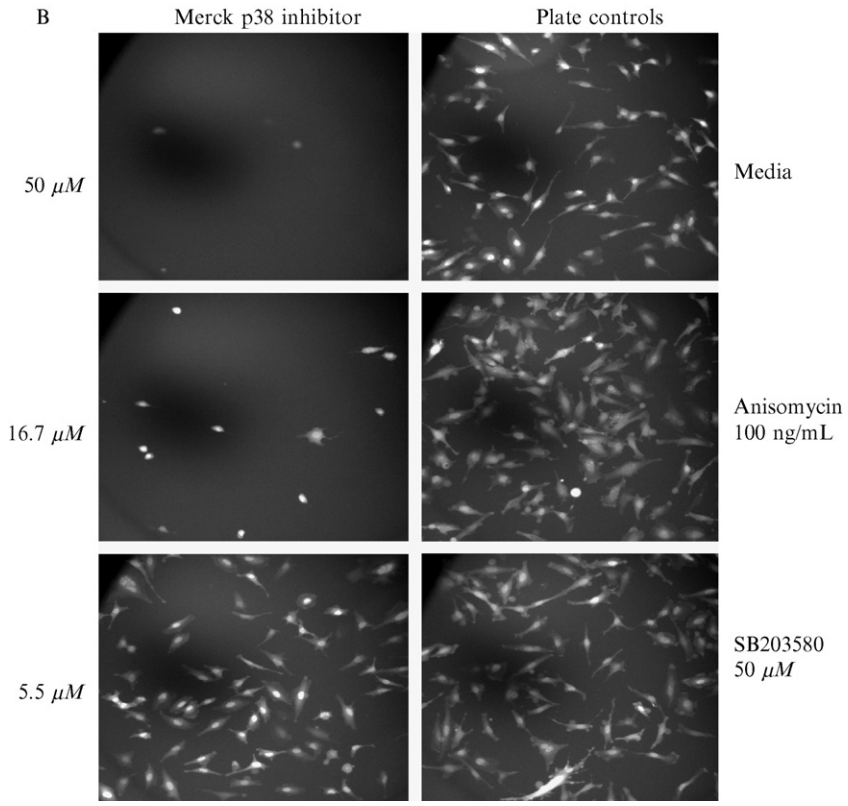

FIG. 9. Secondary analysis of multiparameter image-derived data. The nuclear translocation algorithm provides a range of image-derived features at the individual cell level or at the well averaged level (Table III). The ArrayScan software provides data visualization tools that allow the user to analyze these multiparameter data and the images from which they have been derived. (A) Multiparameter data views. Data views for the valid object counts, the average cell density per field, and the number of valid fields are presented with obvious outliers; data are circled in red. (B) Image views. Representative images captured in wells treated with 50 and 16.6 μM of the p38 Merck inhibitor compared to the 5.5 μM dose, together with images from plate control wells.

likely that the Merck inhibitor compound, at 50 and 16.6 μM, was either cytotoxic or reduced the adherence of the HeLa cells significantly.

Discussion

This chapter described the generation and characterization of a stable MK2-EGFP expressing HeLa cell line and the subsequent development of a high-content imaging assay on the Cellomics ArrayScan platform to

screen for p38 MAPK inhibitors. The assay took advantage of the well-substantiated hypothesis that mitogen-activated protein kinase-activating protein kinase-2 is a substrate of p38 MAPK kinase and that p38-induced phosphorylation of MK-2 induces a nucleus-to-cytoplasm translocation (Engel *et al.*, 1998; Neininger *et al.*, 2001; Zu *et al.*, 1995).

Through a process of heterologous expression of a MK2-EGFP fusion protein in HeLa cells using retroviral infection, antibiotic selection, and flow sorting, we were able to isolate a MK2-EGFP-HeLa cell line in which the MK2-EGFP translocation response could be robustly quantified on the Cellomics ArrayScan HCS platform (Figs. 1–4, Table I). Several clonal populations were isolated from the original retrovirus-infected population by flow sorting and selection, and their GFP expression and intensity levels were measured by FACS analysis (Table I) and compared to their anisomycin-induced MK2-EGFP translocation responses (Figs. 3 and 4). Five of the six cell lines produced a dose-dependent anisomycin-induced MK2-EGFP translocation response (Fig. 4). Only the highest-expressing cell line, the C5 clone, which was 80% positive for EGFP expression with an MFI of 266, failed to exhibit an anisomycin-induced MK2-EGFP translocation response (Fig. 4). The A4 clone of MK2-EGFP-HeLa cells, which was 78% positive for EGFP expression with an MFI of 105 (Table I), was selected for further assay development because it exhibited the most robust assay signal window for anisomycin-induced MK2-EGFP translocation (Fig. 4). Similar responses were observed when TNFα was used as the stimulus to activate the p38 MAPK pathway (data not shown). The characterization and selection of the appropriate clone or cell line were the most critical steps of the assay development process. Overexpression of the fusion protein in the A4-MK2-EGFP-HeLa cell population had no effect on the qualitative pattern of the p38 and MK2 phosphorylation responses to p38 MAPK activation induced by anisomycin, although there was an apparent overall increase in phospho-p38 and phospho-MK2 signal strength relative to wild-type HeLa cells (Fig. 5).

The A4-MK2-EGFP-HeLa cell line was used to develop an assay for identifying p38 inhibitors that would be compatible with HTS on the Cellomics ArrayScan imager. A series of experiments were conducted to optimize the assay with respect to cell seeding density, length of anisomycin stimulation, DMSO tolerance, assay signal window, and reproducibility (Figs. 6–8). The resulting MK2-EGFP translocation assay was compatible with HTS and was shown to be an effective cell-based assay to identify p38 inhibitors (Fig. 7B, Table II). p38 has been a major target for drug discovery by the pharmaceutical industry, as indicated by the numerous patent applications and small molecule inhibitors that have been developed (English and Cobb, 2002; Fabbro *et al.*, 2002; Noble *et al.*, 2004; Regan

et al., 2002). Many of these p38 inhibitors have exhibited significant efficacy in cellular assays and animal disease models and several have progressed into human clinical trails for the treatment of inflammation and cancer (English and Cobb, 2002; Fabbro *et al.*, 2002; Noble *et al.*, 2004; Regan *et al.*, 2002). For example, SB203580 and BIRB 796 and their analogs have been shown to be potent and selective inhibitors of p38 MAPK (English and Cobb, 2002; Fabbro *et al.*, 2002; Noble *et al.*, 2004; Regan *et al.*, 2002). SB203580 and BIRB 796 produced IC_{50} values of 60 and 18 n*M,* respectively, in a THP-1 TNFα production cell model (Regan *et al.*, 2002). In the MK2-EGFP translocation assay described here, SB203580 produced an IC_{50} of 53 nM, and the other published p38 inhibitors produced IC_{50} values below 100 n*M*. In a similar MK2-GFP redistribution assay developed in a BHK-1 cell background and quantified on the In cell analyzer 3000 imaging platform, SB203580 produced an IC_{50} of 3.4 μM for anisomycin-induced redistribution (Almholt *et al.*, 2004), ~60-fold less sensitive than the assay described here. The BHK-1 MK2 redistribution assay was utilized for an HTS of 183,375 compounds that identified two main classes of inhibitors: direct inhibitors of the MK2 nuclear export process and inhibitors of the upstream p38 MAPK pathway (Almholt *et al.*, 2004). Hits from the primary screen were categorized via a number of secondary assays and compounds were identified that both structurally and functionally resembled p38 kinase inhibitors (Almholt *et al.*, 2004). In the MK2-EGFP translocation assay described here, neither the PI3-kinase inhibitor wortmannin nor the JNK-1/2 inhibitor SP 600125 inhibited anisomycin-induced MK2-EGFP translocation, indicating some degree of selectivity (Table II). However the MK2-EGFP translocation assay was susceptible to inhibition by the nonselective kinase inhibitor staurosporin, which produced an IC_{50} of 0.75 μM. The MEK-1/2 inhibitors UO126 and PD 98059, produced IC_{50} values of 33 and 39 μM, respectively, perhaps indicating that ERK1/2 may be capable of phosphorylating MK2 as well as MK1, or perhaps reflecting the cross talk between the different modules of MAPK signaling pathways (Cowan and Storey 2003; Garrington and Johnson, 1999). In addition to p38 inhibitors, the MK2-EGF translocation response may therefore be susceptible to other classes of inhibitors: nonselective kinase inhibitors, kinase inhibitors that inhibit upstream kinases in the p38 MAPK signaling pathway, kinases involved in the cross talk between different modules (ERKs, JNKs, and p38s) of the MAPK signaling pathways, and inhibitors of the MK2 nuclear export process. Trask *et al.* (2006) describe the conversion of this assay to a 384-well format and optimization of the assay for the screening of a 32K kinase-biased library to identify p38 MAPK inhibitors.

Some 518 protein kinases encoded in the human genome share a catalytic domain, the ATP-binding site, conserved in sequence and structure (English and Cobb, 2002; Noble *et al.*, 2004). The vast majority of known kinase inhibitors was found to be competitive with ATP, and thus are believed to interact within the ATP-binding site (English and Cobb, 2002; Noble *et al.*, 2004). The conservation of the ATP-binding site within the kinase family and the large number of cellular proteins that bind and/or utilize ATP, together with intracellular concentrations of ATP reported in the millimolar range, raise significant concerns about inhibitor potency in cellular assays, kinase selectivity, and adverse effects (English and Cobb, 2002; Noble *et al.*, 2004). In addition to the direct target readout that can be obtained from the images, the image analysis algorithm also measures and reports multiple features and image-based parameters that provide information on cell morphology, cytotoxicity, and potential interference by fluorescent compounds (Giuliano *et al.*, 1997). Thus, by mining these ''high-content'' data it is possible to extract additional information on the effects of compound treatment of cells (Fig. 9). For example, we observed that the two highest concentrations of the Merck p38 inhibitor compound were producing obvious outliers in several parameters relative to the other wells on the plate (Fig. 9A). A visual inspection of the images revealed that there were fewer cells in the fields of view captured from wells treated with 50 and 16.6 μM of the Merck inhibitor compared to the 5.5 μM dose or images from control wells (Fig. 9B). The Merck p38 inhibitor compound produced an IC_{50} of 7 nM in the MK2-EGFP translocation assay, but at 50 and 16.6 μM doses was either cytotoxic or significantly reduced the adherence of the HeLa cells. While the acute effects on cytotoxicity or cell morphology observed in our MK2-EGFP HeLa cell-based model may not be predictive of *in vivo* toxicity, it is important to note that a number of the p38 inhibitors, including the Merck p38 inhibitor, have been withdrawn from clinical trials because of adverse toxicity profiles (English and Cobb, 2002; Fabbro *et al.*, 2002; Noble *et al.*, 2004; Regan *et al.*, 2002). It will be interesting to see whether the ability of HCS to measure and discriminate between the on-target and off-target effects of lead compounds will provide cell-based models that will improve the conversion rate of drug candidates to successful drugs.

References

Almholt, D. L., Loechel, F., Nielsen, S. J., Krog-Jensen, C., Terry, R., Bjorn, S. P., Pedersen, H. C., Praestegaard, M., Moller, S., Heide, M., Pagliaro, L., Mason, A. J., Butcher, S., and Dahl, S. W. (2004). Nuclear export inhibitors and kinase inhibitors identified using a MAPK-activated protein kinase 2 redistribution screen. *Assay Drug Dev. Technol.* **2,** 7–20.

Cowan, K. J., and Storey, K. B. (2003). Mitogen-activated protein kinases: New signaling pathways functioning in cellular responses to environmental stress. *J. Exp. Biol.* **206,** 1107–1115.

DeBiasio, R., Bright, G. R., Ernst, L. A., Waggoner, A. S., and Taylor, D. L. (1987). Five-parameter fluorescence imaging: Wound healing of living Swiss 3T3 cells. *J. Cell Biol.* **105,** 1613–1622.

Engel, K., Kotlyarov, A., and Gaestel, M. (1998). Leptomycin B-sensitive nuclear export of MAPKAP kinase 2 is regulated by phosphorylation. *EMBO J.* **17,** 3363–3371.

English, J. M., and Cobb, M. H. (2002). Pharmacological inhibitors of MAPK pathways. *Trends Pharmacol. Sci.* **23,** 40–45.

Fabbro, D., Ruetz, S., Buchdunger, E., Cowan-Jacob, S. W., Fendrich, G., Liebetanz, J., Mestan, J., O'Reilly, T., Traxler, P., Chaudhuri, B., Fretz, H., Zimmermann, J., Meyer, T., Caravatti, G., Furet, P., and Manley, P. W. (2002). Protein kinases as targets for anticancer agents: From inhibitors to useful drugs. *Pharmacol. Ther.* **93,** 79–98.

Garrington, T. P., and Johnson, G. L. (1999). Organization and regulation of mitogen activated protein kinase signaling pathways. *Curr. Opin. Cell Biol.* **11,** 211–218.

Giuliano, K. A., DeBiasio, R. L., Dunlay, R. T., Gough, A., Volosky, J. M., Zock, J., Pavlakis, G. N., and Taylor, D. L. (1997). High-content screening: A new approach to easing key bottlenecks in the drug discovery process. *J. Biomol. Screen.* **2,** 249–259.

Giuliano, K. A., and Taylor, D. L. (1998). Fluorescent-protein biosensors: New tools in drug discovery. *TIBTech.* **16,** 135–140.

Johnston, P. A., and Johnston, P. A. (2002). Cellular platforms for HTS: Three case studies. *Drug Discov. Today* **7,** 353–363.

Kotlyarov, A., Neininger, A., Schubert, C., Eckert, R., Birchmeier, C., Volk, H. D., and Gaestel, M. (1999). MAPKAP kinase 2 is essential for LPS-induced TNF-alpha biosynthesis. *Nature Cell Biol.* **1,** 94–97.

Lundholt, B. K., Linde, V., Loechel, F., Pedersen, H. C., Moller, S., Praestegaard, M., Mikkelsen, I., Scudder, K., Bjorn, S. P., Heide, M., Arkhammar, P. O., Terry, R., and Nielsen, S. J. (2005). Identification of Akt pathway inhibitors using redistribution screening on the FLIPR and the IN Cell 3000 analyzer. *J. Biomol. Screen.* **10,** 20–29.

Mitchison, T. J. (2005). Small-molecule screening and profiling by using automated microscopy. *Chembiochem.* **6,** 33–39.

Neininger, A., Kontoyiannis, D., Kotlyarov, A., Winzen, R., Eckert, R., Volk, H. D., Holtmann, H., Kollias, G., and Gaestel, M. (2002). MK2 targets AU-rich elements and regulates biosynthesis of tumor necrosis factor and interleukin-6 independently at different post-transcriptional levels. *J. Biol. Chem.* **277,** 3065–3068.

Neininger, A., Thielemann, H., and Gaestel, M. (2001). FRET-based detection of different conformations of MK2. *EMBO Rep.* **2,** 703–708.

Noble, M. E. M., Endicott, J. A., and Johnson, L. N. (2004). Protein kinase inhibitors: Insights into drug design and structure. *Science* **303,** 1800–1805.

Ono, K., and Han, J. (2000). The p38 signal transduction pathway, activation and function. *Cell. Signal.* **12,** 1–13.

Ramm, P., Alexandrov, Y., Cholewinski, A., Cybuch, Y., Nadon, R., and Soltys, B. J. (2003). Automated screening of neurite outgrowth. *J. Biomol. Screen.* **8,** 7–18.

Regan, J., Breitfelder, S., Cirillo, P., Gilmore, T., Graham, A. G., Hickey, E., Klaus, B., Madwed, J., Moriak, M., Moss, N., Pargellis, C., Pav, S., Proto, A., Swinamer, A., Tong, L., and Torcellini, C. (2002). Pyrazole urea-based inhibitors of p38 MAP kinase: From lead compound to clinical candidate. *J. Med. Chem.* **45,** 2994–3008.

Roessel, P. V., and Brand, A. H. (2001). Imaging into the future: Visualizing gene expression and protein interactions with fluorescent proteins. *Nature Cell Biol.* **4,** E15–E20.

Tavare, J. M., Fletcher, L. M., and Welsh, G. I. (2001). Using green fluorescent protein to study intracellular signaling. *J. Endocrinol.* **170,** 297–306.

Thomas, N., and Goodyer, D. (2003). Stealth sensors: Real-time monitoring of the cell cycle. *Targets* **2,** 26–33.

Trask, O. J., Jr., Baker, A., Williams, R. G., Kickischer, D., Kandasamy, R., Laethem, C., Johnston, P. A., and Johnston, P. A. (2006). Assay development and case history of a 32K-biased library high-content MK2-EGFP translocation screen to identify p38 MAPK inhibitors on the ArrayScan 3.1 imaging platform. *Methods Enzymol.* **414** (this volume).

Zhang, J. H., Chung, T. D., and Oldenburg, K. R. (1999). A simple statistical parameter for use in evaluation and validation of high throughput screening assays. *J. Biomol. Screen.* **4,** 67–73.

Zu, Y. L., Ai, Y., and Huang, C. K. (1995). Characterization of an autoinhibitory domain in human mitogen-activated protein kinase-activated protein kinase 2. *J. Biol. Chem.* **270,** 202–206.

[22] Development and Implementation of Three Mitogen-Activated Protein Kinase (MAPK) Signaling Pathway Imaging Assays to Provide MAPK Module Selectivity Profiling for Kinase Inhibitors: MK2-EGFP Translocation, c-Jun, and ERK Activation

By DEBRA NICKISCHER, CARMEN LAETHEM, OSCAR J. TRASK, JR., RHONDA GATES WILLIAMS, RAMANI KANDASAMY, PATRICIA A. JOHNSTON, and PAUL A. JOHNSTON

Abstract

This chapter describes the development and implementation of three independent imaging assays for the major mitogen-activated protein kinase (MAPK) signaling modules: p38, JNK, and ERK. There are more than 500 protein kinases encoded in the human genome that share an ATP-binding site and catalytic domain conserved in both sequence and structure. The majority of kinase inhibitors have been found to be competitive with ATP, raising concerns regarding kinase selectivity and potency in an environment of millimolar intracellular concentrations of ATP, as well as the potential for off-target effects via the many other cellular proteins that bind and/or utilize ATP. The apparent redundancy of the kinase isoforms and functions in the MAPK signaling modules present additional challenges for kinase

METHODS IN ENZYMOLOGY, VOL. 414 0076-6879/06 $35.00

DOI: 10.1016/S0076-6879(06)14022-7